Contents

Contributors to Volume III v
Preface vii

1. Magnetism and Crystal Structure in Nonmetals

John B. Goodenough

I. Some Important Nonmetallic Structures 1
II. Description of Outer Electrons 24
III. Applications to Magnetism 37
References 59

2. Evaluation of Exchange Interactions from Experimental Data

J. Samuel Smart

I. Introduction 63
II. Isolated Clusters 67
III. Antiferromagnetic Compounds 84
IV. Ferrimagnetic Compounds 103
V. Miscellaneous Comments and Conclusions 107
VI. Recent Developments 108
Appendix A. Molecular Field Relations 111
References 112

3. Theory of Neutron Scattering by Magnetic Crystals

P. G. de Gennes

I. Introduction 115
II. Basic Formulas for "Spin-Only" Magnetic Moments . . 117
III. Diffuse Scattering in the Quasistatic Approximation . . . 127

IV. Inelastic Collisions 136
V. Effects of Orbital Magnetism 142
References 146

4. Spin Configuration of Ionic Structures: Theory and Practice

E. F. Bertaut

Introduction 150
I. Theoretical; the Macroscopic Theory 150
II. Theoretical; the Microscopic Method (Matrix Method) . 160
III. Practice 179
Appendix A. Decomposition of $W_{RR'}$ 198
Appendix B. Some Remarks on Dipolar Energy 199
Appendix C. Some Remarks on the Lyons-Kaplan and Other Methods 201
References 205

5. Spin Arrangements in Metals

R. Nathans and S. J. Pickart

I. Introduction 211
II. Neutron Diffraction Techniques 212
III. Spin Structures 219
IV. Magnetic Form Factors and Spin Densities 247
V. Conclusion 265
References 267

6. Fine Particles, Thin Films and Exchange Anisotropy (Effects of Finite Dimensions and Interfaces on the Basic Properties of Ferromagnets)

I. S. Jacobs and C. P. Bean

I. Introduction 271
II. Fine Particles; Superparamagnetism 272
III. Thin Films 298
IV. Surface Anisotropy 314
V. Exchange Anisotropy 323
References 344

7. Permanent Magnet Materials

E. P. Wohlfarth

I. Introduction 351
II. Theory of Permanent Magnets as Fine Particle Materials . 353
III. Permanent Magnet Powder Materials 372
IV. Permanent Magnet Alloys 379
References 390

8. Micromagnetics

S. Shtrikman and D. Treves

I. Introduction 395
II. Brown's Equations 396
III. Solutions of Brown's Equations 399
IV. Discussion 409
References 413

9. Domains and Domain Walls

J. F. Dillon, Jr.

I. Introduction 415
II. Observation of Domain Structure 416
III. Domain Structures 429
IV. Domain Walls 442
V. Antiferromagnetic Domains 453
VI. Films and Teaching Aids 459
References 461

10. The Structure and Switching of Permalloy Films

Donald O. Smith

I. Introduction 465
II. Preparation and Structure 468
III. Quasistatic Switching 482
IV. Pulse Switching 505
Appendix A. Dispersion Measurements 517
Appendix B. Notation for Applied Fields 520
References 521

11. Magnetization Reversal in Nonmetallic Ferromagnets

E. M. Gyorgy

I. Introduction 525
II. Experimental Procedures and Results 529
III. Equation of Motion of the Magnetization 532
IV. Modes of Magnetization Reversal 538
V. Conclusion 550
References 551

12. Preparation and Crystal Synthesis of Magnetic Oxides

C. J. Kriessman and N. Goldberg

I. Polycrystalline Materials 553
II. Preparation of Single Crystals 580
References 595

Author Index 599
Subject Index 615

1. Magnetism and Crystal Structure in Nonmetals

John B. Goodenough

*Lincoln Laboratory**
Massachusetts Institute of Technology,
Lexington, Massachusetts

I. Some Important Nonmetallic Structures 1
1. Cubic Structures 2
2. Hexagonal Structures 14
3. Tetragonal Structures: Rutile (TiO_2) 22
II. Description of Outer Electrons 24
1. The Free Atom 24
2. Solids 26
III. Applications to Magnetism 37
1. Site Preference Energies 37
2. Electron Ordering Transitions 47
References 59

I. Some Important Nonmetallic Structures

Crystal structure must be considered whenever the relationship between chemistry and a particular phenomenological, magnetic parameter is desired. Although the design of practical materials requires consideration of many extrinsic structural parameters—such as shape and size of the specimen or the shape, size, orientation, distribution, and intrinsic character of impurities or imperfections—these aspects of structure are not considered in this chapter. Further, the relationship between the intrinsic aspects of structure that are discussed here and specific magnetic phenomena is made in those chapters where these phenomena are discussed. For example, the relationship of structure to crystalline anisotropy and magnetostriction is given in Chapter 4

* Operated with support from the U. S. Army, Navy, and Air Force.

of Volume I; the structure dependence of weak ferromagnetism due to an anisotropic superexchange that cants the atomic moments is given in Chapter 3 of Volume I; magnetic order, which depends upon the number and symmetrical arrangement of near neighbors as well as the relative strengths of the couplings between them, is discussed in Chapters 4 and 5 of this volume; and the structural dependence of the magnetic coupling between neighboring atomic moments is discussed in Chapter 2 of this volume, as well as in Chapter 2 of Volume I and in Volume II. Therefore this chapter is confined to a description of several important, nonmetallic structures (Section I) and of the types of distortion that may be encountered in these structures as a result of electron ordering (Section III). In order to discuss the various types of cation and electron ordering that are encountered, it is necessary to review briefly (Section II) two descriptions of the outer electrons and the domain of applicability of each.

1. Cubic Structures

a. Rocksalt, zincblende, and antifluorite. Frequently the ions or atoms of a compound are so arranged that one constituent forms a close-packed array. In Fig. 1 is shown the cubic close-packed (fcc) lattice.

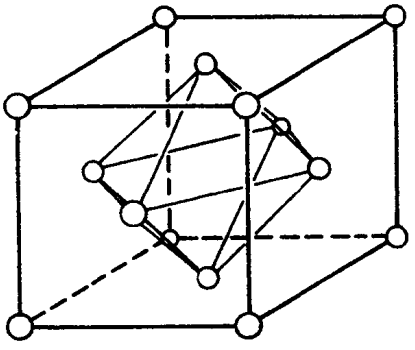

FIG. 1. The face-centered cubic lattice with inscribed octahedral interstice. Eight tetrahedral interstices are defined by the eight octahedral faces and the respective corner atoms toward which they face.

It contains two types of interstices: octahedral with coordination six and tetrahedral with coordination four. It is apparent from Fig. 1 that interstices of the same type share common edges and corners; those of different type, common faces. The octahedral interstices, which are located at the body-center and cube-edge positions, also form a fcc lattice whereas the tetrahedral sites, which are twice as numerous, form a simple cubic lattice.

(1) *Rocksalt.* In the rocksalt structure, the cations occupy the octahedral interstices of a fcc anion sublattice. This gives two interpenetrating fcc sublattices with each ion of one sublattice having six octahedral near neighbors of the other, and twelve next-nearest neighbors of its own. This structure illustrates several features of importance for magnetism.

Phase stability: For primarily ionic compounds, the principal binding forces responsible for phase stability may be obtained from an electrostatic calculation in which the structure is assumed to be composed of charged spheres. There are, however, important corrections that must be made. For example, if there is a large electronegativity difference between sublattices and a small ($\lesssim$0.414) cation:anion size ratio, then additional anion-anion repulsive forces become important [1]. Of more direct significance for magnetism are corrections to this model that must be applied if there are partially filled outer electron shells on the cations. Electron ordering in these partially filled shells destroys the spherical symmetry of the cation and therefore introduces crystallographic distortions to permit close packing of the "aspherical balls." These distortions are discussed in Section III.

Magnetic interactions: In addition these partially filled outer electron shells may have significant interactions with one another, especially if the outer electrons are *d* electrons. There are two types of intercation interaction that can be distinguished: cation- -cation interactions, which are inhibited by anion-sublattice shielding, and cation-anion-cation interactions, in which the anion sublattice plays the role of an intermediary. Cation- -cation interactions may occur if the neighboring cations occupy interstices that share either a common face or a common edge. If they are strong, they cause the outer *d* levels to broaden into a band of collective electron states (see Section II); and if they are weak they introduce superexchange interactions that would correlate the cation spins. Cation-anion-cation interactions also introduce superexchange interactions that would correlate the spins of the cations, in this case, the spins of the cations that share a common near-neighbor anion. Maximum interactions occur for cation-anion-cation angles of 180°, minimum for angles of 90° (Volume I, Chapter 2).

Magnetic order: With from five to eight outer 3*d* electrons, the outer 3*d* electrons of a rocksalt compound are generally localized and the dominant intercation interactions responsible for the magnetic order are 180° cation-anion-cation interactions. The fcc cation sublattice is composed of four interpenetrating, simple cubic sublattices; and the 180° cation-anion-cation interactions only couple the atomic moments within a simple cubic sublattice. Some weaker interaction must be

responsible for whatever coupling there is between these sublattices. Cooperative spin-orbit distortions (see Section III) stabilize collinear spin configurations in FeO and CoO; in MnO and NiO the magnetostrictive forces are much weaker, and multidomain (but apparently not multi-spin-axis) configurations are observed [2] that are compatible with the configurational degeneracy for dipole-dipole interactions [3, 4]. (Any magnetic exchange energy between cation nearest neighbors is cancelled out if the predominant, 180° cation-anion-cation interaction is antiferromagnetic.)

(2) *Zincblende* (*sphalerite*). In the zincblende and antifluorite structures, cations occupy the tetrahedral interstices. In zincblende half the tetrahedral interstices are filled in an ordered manner to form a fcc sublattice. In this case the two interpenetrating, fcc sublattices have tetrahedral near-neighbor coordination. The near-neighbor cations occupy interstices that share only a common corner, and the next-near-neighbor cations are coupled only via two intermediary anions. Therefore, in this structure the strong exchange interactions must be between nearest-neighbor cations. Since it is not possible to propagate antiferromagnetic order between nearest neighbors of a close-packed array, some compromise configuration that permits eight antiferromagnetic and four ferromagnetic couplings occurs whenever this cation-anion-cation interaction is antiferromagnetic. Which of several alternatives is realized in fact depends upon secondary forces, such as the dipole-dipole interactions. (Keffer [4a] has pointed out that, if anisotropic superexchange is included in the spin-dependent Hamiltonian, the compromise ground state of cubic β-MnS is a spiral ($\theta = 90°$) propagating along a [100], but with antiferromagnetic, collinear (001) planes).

Chalcopyrite, $CuFeS_2$, has the zincblende structure, but with ordering of the Cu^+, Fe^{3+} ions within (001) layers so that the paramagnetic Fe^{3+} cation has only four tetrahedral Fe^{3+} near neighbors, but eight diamagnetic Cu^+ near neighbors. In this structure antiferromagnetic order can be propagated unambiguously over the Fe^{3+} sublattice. Cation ordering distorts the symmetry from cubic to tetragonal.

(3) *Antifluorite*. The antifluorite structure has all of the tetrahedral sites filled with cations, and cation- -cation exchange interactions may be competitive with cation-anion-cation interactions. In fact, the intercation separation may be sufficiently small that cation $3d$ electrons are collective rather than localized. *Fluorite*, CaF_2, has a structure in which the cation and anion sublattices are just reversed.

The Li_3Bi structure has all of the interstices, both octahedral and tetrahedral, filled with Li^+ ions.

b. ReO_3 and perovskite, $CaTiO_3$. If one of the simple cubic sublattices is removed from the fcc anion array, the anion sublattice is that of the ideal ReO_3 structure. Removal of a simple cubic anion sublattice destroys three out of four of the octahedral interstices, and the Re^{6+} ions are located in the remaining simple cubic sublattice of octahedral sites. Thus the cations form a simple cubic array, and the anions are located at the centers of the cube edges. The trifluorides CrF_3, FeF_3, CoF_3, and MoF_3 are of similar structure, but with a distortion to rhombohedral symmetry. With more ionic bonds, the structure is stabilized by the closer packing of the ions at the expense of distortions from cubic symmetry. In the transition metal fluorides, the cation-anion-cation angle is $\sim 154°$ instead of 180° and the cation cube is stretched along a [111].

In the ideal perovskite ABX_3, the missing anions of the ReO_3 structure are replaced by large cations A so that the AX_3 sublattice is fcc. This obviously puts a restriction on the relative sizes of the various ions that stabilize this structure. Goldschmidt [5] has defined a tolerance factor $t = (r_A + r_B)/[\sqrt{2}(r_B + r_X)]$, where r_A, r_B, r_X are Goldschmidt radii of the respective ions. Stabilization of the perovskite phase appears to require roughly $0.8 < t < 1.0$. For lower values of t, the ilmenite or corundum structure is formed. Further, three out of four of the octahedral sites and all the tetrahedral sites are coordinated by an A cation, so that electrostatic forces keep them free of B cations. Therefore the B cations are located in the remaining simple cubic sublattice of all-anion-coordinated octahedral sites. Thus the ideal cubic perovskite is made up of a simple cubic sublattice of B cations with A cations located at the body centers and anions at the centers of the cube edges.

If only the B cations are paramagnetic, only 180° cation-anion-cation superexchange interactions are present in either ReO_3 or perovskite structures. Therefore compounds and systems with these structures have been extensively studied in order to test the validity of various superexchange theories [6].

In practice, the ideal cubic perovskite is rarely encountered in nature, the mineral $CaTiO_3$ itself having a larger unit cell due to a cooperative buckling of the anion octahedra to permit closer packing of the ions. This enlarged unit cell is more prevalent in perovskites with a relatively small A cation. A detailed description of the unit cell has been supplied by Geller's [7] x-ray study of single crystals of $GdFeO_3$. The Fe^{3+} ion has a half-filled *d* shell, the Gd^{3+} a half-filled *f* shell; therefore they do not introduce Jahn-Teller or spin-orbit distortions. $GdFeO_3$ has an orthorhombic structure that is characteristic of most of the perovskites in which the cooperative buckling of anion octahedra occur. The unit

cell is shown in Fig. 2. With probable space group $D_{2h}(16)$-Pb_{nm}, the general solution for the orthorhombic structure gives A cations in positions 4(*c*): $\pm(x, y, 1/4;\ 1/2, -x, 1/2 + y, 1/4)$, the B cations in positions 4(*b*): (1/2, 0, 0; 1/2, 0, 1/2; 0, 1/2, 0; 0, 1/2, 1/2), eight anions X_{II} in 8(*d*): $\pm(x, y, z;\ 1/2 - x, 1/2 + y,\ 1/2 - z;\ \bar{x}, \bar{y}, 1/2 + \bar{z};\ 1/2 + x, 1/2 - y, \bar{z})$, and the remaining four anions X_I in 4(*c*). Coordinates for the ions in $GdFeO_3$ are given in Fig. 2.

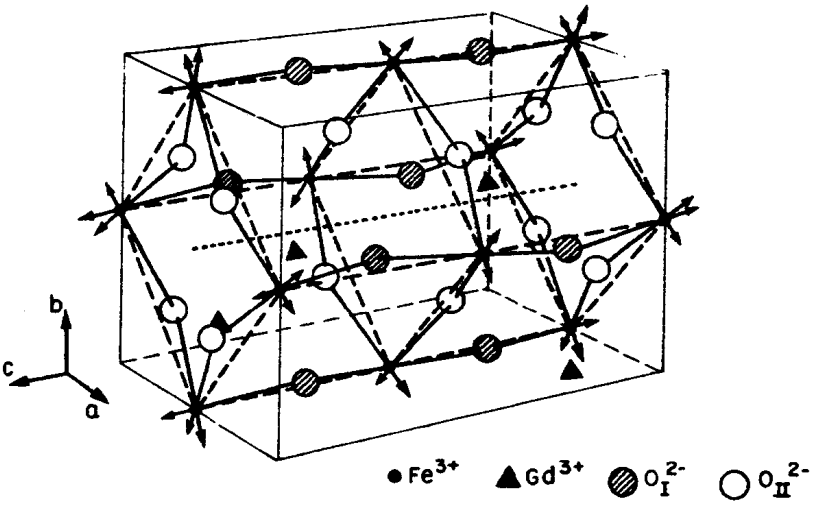

ION	POSITION	COORDINATES x	y	z
Gd^{3+}	4 (c)	-0.018	0.060	1/4
Fe^{3+}	4 (b)	1/2	0	0
O_I^{2-}	4 (c)	0.05	0.470	1/4
O_{II}^{2-}	8 (d)	-0.29	0.275	0.05

FIG. 2. The unit cell of the *O*-orthorhombic perovskite $GdFeO_3$. Extra anions are included to show the cooperative buckling of the anion octahedra.

Powder photographs taken with CrKα radiation indicate the existence of a monoclinic pseudocell containing a single $GdFeO_3$ molecule. The edges of this pseudocell are aligned along the [110], [$\bar{1}$10], and [001] directions of the true orthorhombic cell (see Fig. 2) and $a = c > b$ where $b_{\text{pseudocell}}$ has the same direction as $c_{\text{true cell}}$. Four of these pseudocells (four formula weights) are required for each true cell. It should be noted also that the true orthorhombic cell is characterized by $a < c/\sqrt{2} < b$. Orthorhombic structures of this type should be

distinguished from those with $c/\sqrt{2} < a < b$, which reflect a Jahn-Teller distortion of the octahedral interstices superposed on the puckering (see Section III), even though the space group remains $D_{2h}(16)$-Pb_{nm}. The former class of structures have been designated *O*-orthorhombic, the latter *O'*-orthorhombic [6].

Since the sign of the cation-anion-cation superexchange interactions may change as the angle changes from 180° to 90°, it is important to consider the cation-anion-cation angle. Gilleo [8] has estimated that in $La(Co_{0.2}Mn_{0.8})O_3$ these angles are $180° > \phi \gtrsim 150°$. Experimentally it is found that these deviations from 180° do not introduce any changes from what is predicted for 180° interactions. However, from a study of the ~125° cation-anion-cation interactions in spinels, it appears that changes do occur for $125° \gtrsim \phi \geq 90°$. This sets the critical angle for applicability of the 180° superexchange rules in the range $125° < \phi_c < 150°$.

Attention is also called to the fact that crystalline anisotropies associated with the puckered octahedra can cant the spins of an antiferromagnetic lattice to give a weak, parasitic ferromagnetism [9]. However, the predominant mechanism for parasitic ferromagnetism in the orthoferrites appears to be anisotropic superexchange (antisymmetric exchange) [9a], a concept first introduced from symmetry arguments for the spin axis relative to the axes of crystal symmetry [9b] (see Volume I, Chapter 3).

If the A cation is so large that octahedral-site puckering does not occur, relative ionic size may give a symmetry that is either cubic or rhombohedral. It is noteworthy that although complete solid solutions of orthorhombic perovskites can be obtained, mixtures of a cubic (or rhombohedral) and an orthorhombic perovskite may result in a miscibility gap. Such miscibility gaps have been observed [10] in the $La(Co, Fe)O_3$ and the $La(Mn, Ni)O_3$ systems.

There are some magnetic, metallic perovskites. These have the ideal cubic structure with a metal AX_3 sublattice and a B sublattice that is interstitial nitrogen or carbon. Examples are ferromagnetic Fe_4N, $NiFe_3N$, $PdFe_3N$, $ZnMn_3C$, $GaMn_3C$, $AlMn_3C$ and ferrimagnetic Mn_4N. It is important to note that the interstitial atoms of these compounds are not ionic, so that the 180° cation-anion-cation superexchange rules do not apply [6].

c. Spinel, $MgAl_2O_4$. In the spinel structure, the fcc anion sublattice has half of its octahedral sites and one-eighth of its tetrahedral sites occupied by cations. Alternate [110] or [$\bar{1}$10] rows of octahedral sites are occupied, the direction of the rows alternating between (001) planes

but similar (001) planes repeating only every fourth plane. Since cubic symmetry is preserved, this gives a cubic unit cell that is double that of Fig. 1 in all three directions. Therefore it is eight times as large and contains 32 anions, 16 octahedral-site cations, and 8 tetrahedral-site cations. The occupied tetrahedral sites are those that have all their near-neighbor octahedral sites empty. The occupied octahedral sites are generally referred to as B sites, the occupied tetrahedral sites as A sites.

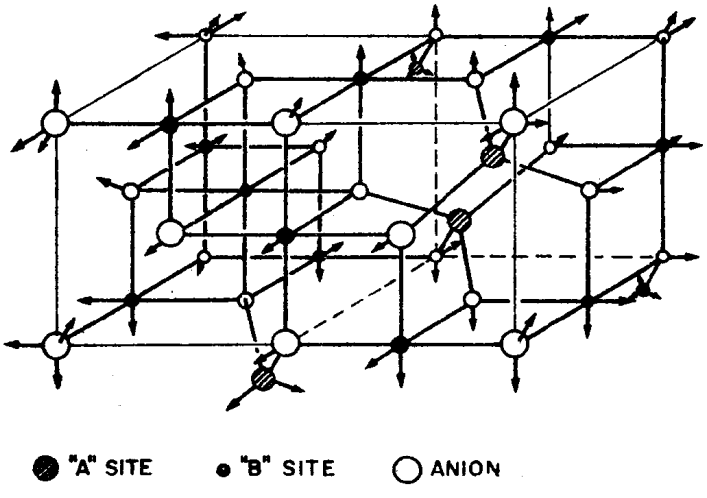

FIG. 3. A primitive unit cell of the spinel lattice as referred to the anion sublattice, which illustrates the fourfold coordination of the anions. Some extra A cations are also shown.

In Fig. 3 are shown two octants of the unit cell as referred to the anion sublattice. Note that each anion has four cation near neighbors: one A and three B. In Fig. 4 are shown the A sites of a unit cell as referred to the A-site sublattice. These form a diamond sublattice. Also shown is a primitive unit cell, which is just two octants of the cubic unit cell, together with the B sites and the anions of this primitive cell. The rest of the B sites and anions of the cubic cell can be obtained by successive translations along the three $< 110 >$ axes. The anions are positioned in the same way in all octants. Each octant contains four anions, which form the corners of a tetrahedron. It follows that the primitive unit cell contains two A sites, four B sites, and eight anions. This gives a total of six cation sublattices that must be considered in any molecular field calculation of the magnetic ordering. Further, it should be noted that each A site is located in purely cubic crystalline fields, whereas each B site has a trigonal field from the cation sublattice superposed on the

cubic fields associated with the anion sublattice. The axis of this trigonal field is parallel to a different $< 111 >$ direction for each of the B sites of the primitive cell, which means that the over-all symmetry of the lattice is cubic. These trigonal fields play an important role in the magnetostriction and crystalline anisotropy of oxide spinels containing V^{3+}, V^{4+}, Co^{2+}, and Fe^{2+} (see Section III; and Chapter 4 of Volume I). They contribute a smaller (higher-order) but important term to the anisotropy of Fe^{3+} or Mn^{2+}.

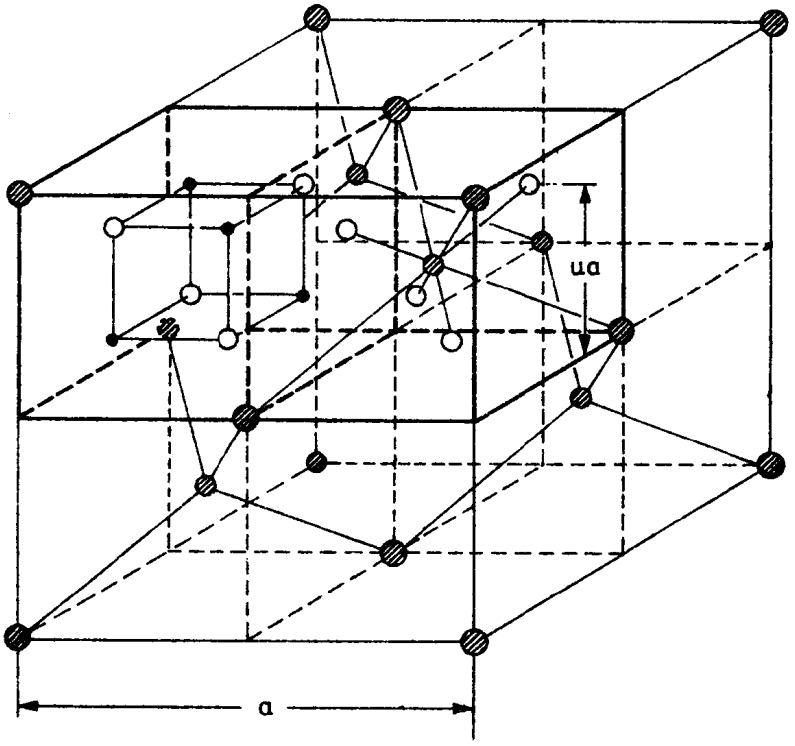

FIG. 4. The A-sublattice unit cell of cubic spinel. A primitive unit cell, which includes anions and B-site cations, is defined by the heavy lines. The spinel u parameter is also defined.

In practice, the anion sublattice suffers small distortions as a result of relative ionic size, but without loss of cubic symmetry. Because the tetrahedral sites are relatively small, most A-site cations are too big to fit in without expanding the site. Unless electron ordering on the A-site cations occurs, this expansion is accomplished by a displacement of the four neighboring anions away from the cation along their bond

axis. The magnitude of this displacement is given by the parameter u, which is defined in Fig. 4. From the definition, $u = \frac{3}{8}$ defines perfect close packing of the anions. It is also apparent from Fig. 4 that expansion ($u > \frac{3}{8}$) of the anion tetrahedra of A-site octants can occur only if there is a simultaneous shrinkage of the anion tetrahedra in the B-site octants. For a hard-sphere model, $R_A + R_0 = (u - \frac{1}{4})a\sqrt{3}$ and $R_B + R_0 = (\frac{5}{8} - u)a$, where R_A and R_B are the ionic radii of the A-site and B-site cations, respectively, and R_0 is the anion radius. If $(R_A + R_0)/(R_B + R_0) > \sqrt{3}/2$, it follows that $u > \frac{3}{8}$. Although the inequality may be reversed in theory, it is rarely reversed in practice. Note also that deviations in u from $\frac{3}{8}$ introduce a trigonal field component to the B-site crystalline fields. Since this anion-sublattice trigonal axis coincides with that due to the cation sublattice, no new crystal field symmetries are introduced. However, the anion-sublattice component has a sign that is opposite that of the cation sublattice, and for a sufficiently large u parameter the sign of the trigonal field component changes.

In the ferrospinels, the dominant magnetic interaction is an antiferromagnetic superexchange coupling (~125° cation-anion-cation) between A-site and B-site cations. This gives rise to Néel ferrimagnetism (collinear spins) with a net spontaneous magnetization that is sensitive to the cation distribution over the A and B sites. Calculation of site preference energies for various cations is discussed in Section III.

In a cubic spinel, antiferromagnetic B-B interactions (90° cation-anion-cation plus cation- -cation) would compete with the A-B interactions. For a sufficiently large B-B interaction, the collinear spin configuration proposed by Néel is no longer stable at low temperatures, the ground-state spin configuration becoming a complex, ferrimagnetic spiral [11]. The relative magnitudes of these interactions depend upon the cation occupation of the A and B sites, so that a knowledge of site preference energies may be important also for prediction of the type of magnetic order to be anticipated in a given spinel.

d. Pyrite. The compound FeS_2 is essentially $Fe^{2+}S_2^{2-}$, an S_2^{2-} molecular ion acting as the anion. The structure is analogous to rocksalt, the cation and molecular-anion sublattices each being fcc. However, the S_2^{2-} molecule has axial, not spherical, symmetry, and it is necessary to further specify the ordering of the S_2^{2-} axes. In Fig. 5 are shown (a) the orientation of the S_2^{2-} molecule in an octahedral cation interstice and (b) the sulfur coordination about a cation. The axis of the S_2^{2-} molecular ion is always along one of the four $< 111 >$ axes such that each sulfur is tetrahedrally coordinated by three cations and another

sulfur. Within a cubic cell, each of the $< 111 >$ directions are equally occupied, so that the symmetry remains cubic. About a given cation the orientations order so as to preserve octahedral near-neighbor coordination for the cation. This structure provides anisotropic superexchange between nearest neighbors, half of the interactions being stronger than the next-near-neighbor interactions, half being the same.

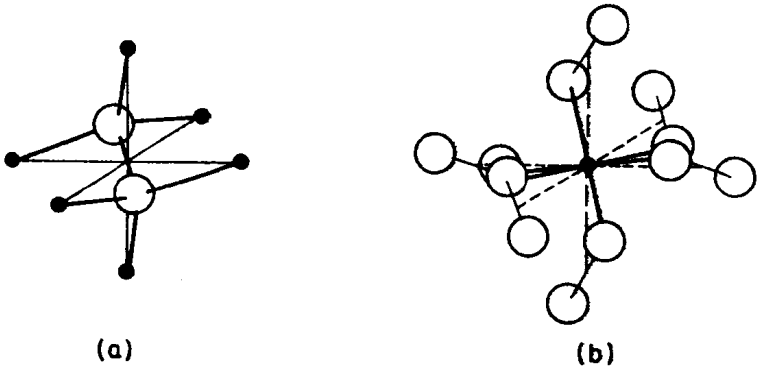

FIG. 5. Anion and cation coordinates in pyrite. (*a*) S_2^{2-} in a cation-sublattice octahedral site. (*b*) Sixfold coordination of a cation by S_2^{2-} molecules.

This is quite different from the rocksalt compounds where, with five or more outer *d* electrons, the near-neighbor interactions are isotropic and weaker than the next-near-neighbor interactions.

e. Garnet, $Mn_3Al_2(SiO_4)_3$. The mineral garnet, $Mn_3Al_2(SiO_4)_3$, is important for magnetism because it is possible to substitute Fe^{3+} for both the Al^{3+} and the Si^{4+}. To do this, it is necessary to have a relatively large trivalent ion substitute for Mn^{2+}. Y^{3+} and the rare earth ions Pm^{3+} through Lu^{3+}, which are all of comparable ionic radius, have been used successfully. The structure is particularly stable, presumably because all of the anion-sublattice interstices are occupied by cations, and the compound can tolerate only small deviations from stoichiometry. This means that, with careful preparation, Fe^{2+}-ion contamination can be made extremely small. This fact is important for microwave devices where dielectric losses due to electron transfer between Fe^{3+} and Fe^{2+} ions are a problem. Also, there is chemical homogeneity in each type of site, and this reduces losses due to spin-lattice interactions (See Volume I, Chapter 10).

The crystal structure is quite complicated. It was first worked out by Menzer [12], but the significance of this structure for ferrimagnetism

was first recognized in Grenoble [12a], where it was discovered that iron—and many other transition-metal ions—can be substituted into it [12b]. Subsequent single-crystal work [13] has permitted quite precise location of the O^{2-} ions in $Y_3Fe_5O_{12}$. This structure is not based on a close-packed anion sublattice. The most important features for magnetism can be obtained from a consideration of the cation sublattice. There are three types of cation sites: tetrahedral, octahedral, and dodecahedral. These are arranged as shown in Fig. 6. The octahedral site cations of an octant of the large unit cell are body-centered

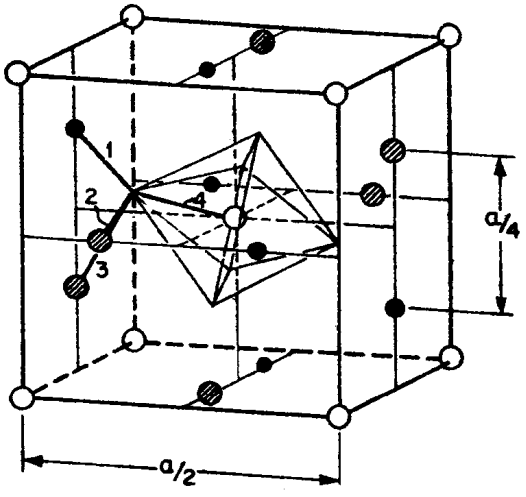

FIG. 6. One octant of the cation-sublattice unit cell of garnet. The anion octahedral coordination about the body-center cation of this octant is also shown, along with the fourfold coordination about the anions.

cubic (bcc). The tetrahedral-site and dodecahedral-site cations alternate along chains that are in the faces of these cubes. On going from one (100) face to the next, the phase of the chain sequence changes, so that it is necessary to double all three edges of the bcc cell to obtain the true unit cell. The O^{2-} octahedron around the body-center cation is also shown in Fig. 6. Each O^{2-} ion has four near neighbors: two dodecahedral cations, one tetrahedral, and one octahedral cation. It is therefore obvious from Fig. 6 that the orientation of the O^{2-} octahedron must alternate on passing from one octant to the next. Further, none of the O^{2-} polyhedra about a cation are regular, but have the dimensions

shown in Fig. 7. However, the $Fe^{3+} - O^{2-}$ distance is constant within an interstice, being 2.00 Å for octahedra and 1.88 Å for tetrahedra in $Y_3Fe_5O_{12}$. These distortions are important for the crystal fields at the cations.

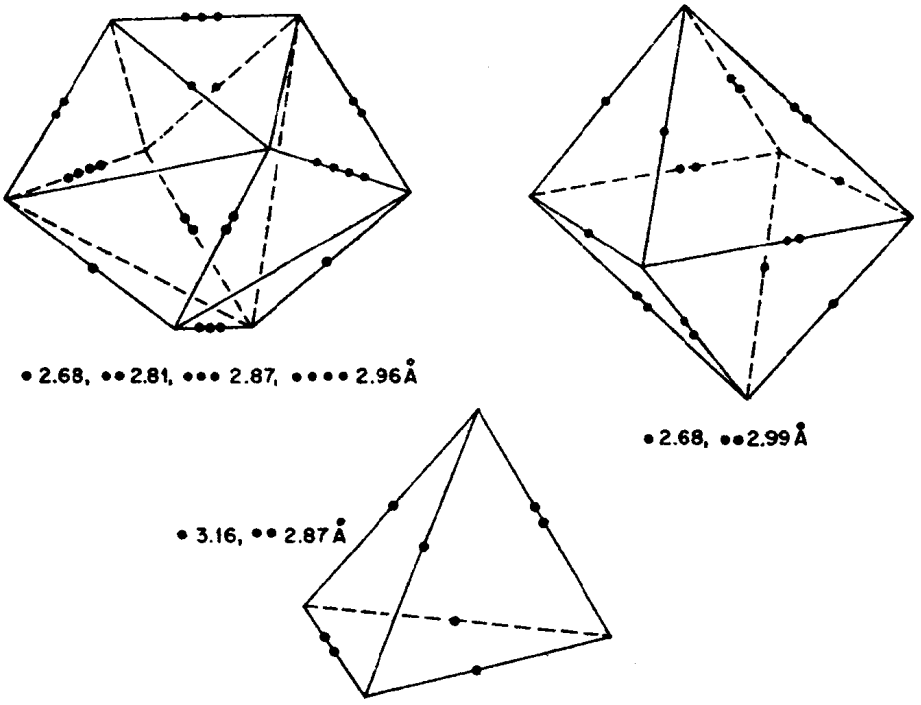

FIG. 7. Symmetry of the dodecahedral, octahedral, and tetrahedral interstices found in garnet.

The tetrahedral-O^{2-}-octahedral angle (1,4 of Fig. 6) in $Y_3Fe_5O_{12}$ is 126.6°, so that strong, antiferromagnetic superexchange interactions occur between the Fe^{3+} ions in these sites, just as for the A-B interactions in spinels. Since there are three-halves as many tetrahedral as octahedral cations, this gives rise to ferrimagnetism. Of the dodecahedral-O^{2-}-Fe^{3+} angles, only one is greater than 105°, viz. 1,2 of Fig. 6. For $Y_3Fe_5O_{12}$ this angle is 122.2°. It should provide, therefore, the dominant superexchange couple (see Volume I, Chapter 2). If a rare-earth ion M^{3+} substitutes for Y^{3+}, the net spin of M^{3+} couples antiparallel with the moment of the tetrahedral-site sublattice, presumably via this cation-anion-cation linkage. (For half- or less filled 4*f* shells, $\mathbf{J} = \mathbf{L} - \mathbf{S}$ and the magnetic moment of M^{3+} is parallel to the tetrahedral-site